Science and Technology Indonesia
e-ISSN:2580-4391 *p*-ISSN:2580-4405
Vol. 9, No. 4, October 2024

Research Paper

Graphene Oxide Nano-Sheets: A Novel Eco-Friendly Approach for Tissue Engineering and Antibacterial Applications in Bone Disease

Hind W. Abdullah[1*], Tahseen H Mubarak[1], Kadhim K. Resan[2]

[1]*Department of Physics, Collage of Science, University of Diyala, Diyala, 34001, Iraq*
[2]*Al-Mustansiriyah University, Faculty of Engineering, Baghdad, 10020, Iraq*
***Corresponding author**: hindwaleed@uodiyala.edu.iq*

Abstract
Obtaining novel scaffolds on bone disease-affected cells with osteoconductivity has recently been the focus of tissue engineering methodologies. Chemical treatment and microwave radiation form a novel strategy to create graphene oxide nanosheets (Gns) that decorate carbon crystal structures. This approach is proven to be eco-friendly. Gns was characterized using "X-ray diffraction, ultraviolet, and Fourier transform infrared spectrophotometers". The XRD spectra confirmed the crystalline structure of Gns. The Gns product was analyzed using "Raman spectroscopy. Transmission electron microscopy and field-emission scanning electron microscopy" exposed few layered surfaces of Gns. The TEM images showed Gns specifically decorated with carbon nanoparticles. The evidence demonstrated the novelty of Gns as a very effective bactericidal agent, suggesting its potential as a future antibacterial agent. Different concentrations of Gns and its derivatives showed different cell viabilities toward various cell lines, demonstrating the dependency of a biocompatible environment for good attachment on MG63 cells.

Keywords
Antibacterial, MG63, Graphene Oxide Nano Sheet, Decoration Carbon Nanoparticles

Received: 1 May 2024, Accepted: 27 June 2024
https://doi.org/10.26554/sti.2024.9.4.806-817

1. INTRODUCTION

A significant area of study in medicine is the application of new therapeutic agents to enhance the effectiveness of therapy. In the past, progress in the nanomaterial domain has offered valuable biocompatible nanostructured materials and nanocomposites that are well-suited for drug delivery systems (Kang et al., 2017; Mohammadrezaei et al., 2018). A bone scaffold is usually necessary for stem cells in bone tissue engineering. Biomaterials are used for bone scaffolds because they provide mechanical support while stimulating new bone development. Scaffolds should be osteoconductive, biodegradable, and low profile. Scaffold construction requires superior mechanical properties, interconnected porosity, and biocompatibility (Kang et al., 2017; Sumathra et al., 2018).

Graphene and its derivatives are highly sought-after by scientists in various domains, including biomedicine, tissue engineering, and other emerging materials. Carbon nanotubes, fullerenes, and graphene are materials that are frequently seen as having great potential (Gürünlü et al., 2022; Zare et al., 2021). Specifically, they enhance the attachment, growth, and specialization of cells during the formation of bone cells (osteoblasts). Graphene's biocompatibility with the biological system is an important issue because of its potential medical applications (Li et al., 2024; Wang et al., 2021). Therefore, it must be thoroughly tested before it could be used in humans. Figure 1 depicts the antimicrobial and osteogenesis-stimulating effects of graphene oxide (GO) nanosheets (Gns) in bone and dental implants (Jia et al., 2016; Kang et al., 2017).

Microbial disinfection via nanotechnology using metal nanoparticles and/or nanocarbons is straightforward, cheap, and adaptable. However, antibacterial nanomedicine is only started to be used in clinical settings (Jiang et al., 2018; Wang et al., 2011). Graphene-based materials are commonly utilized to treat bone infections due to their potent antibacterial properties (Suresh and Sivasamy, 2018; Szunerits and Boukherroub, 2016). Removing bacterial biofilms from tissue-engineered scaffolds improves osteoblast adhesion and proliferation, allowing Gns to fight infection while maximizing their osteogenic qualities (Wang et al., 2020; Wu et al., 2021).

Gns has remarkable physical qualities, biocompatibility, and chemical stability, making it one of the most promising carbon derivatives in material science. First discovered in 2004, GO is a monotonically thick, two-dimensional (2D) planar sheet. Researchers have reported several biological and physi-

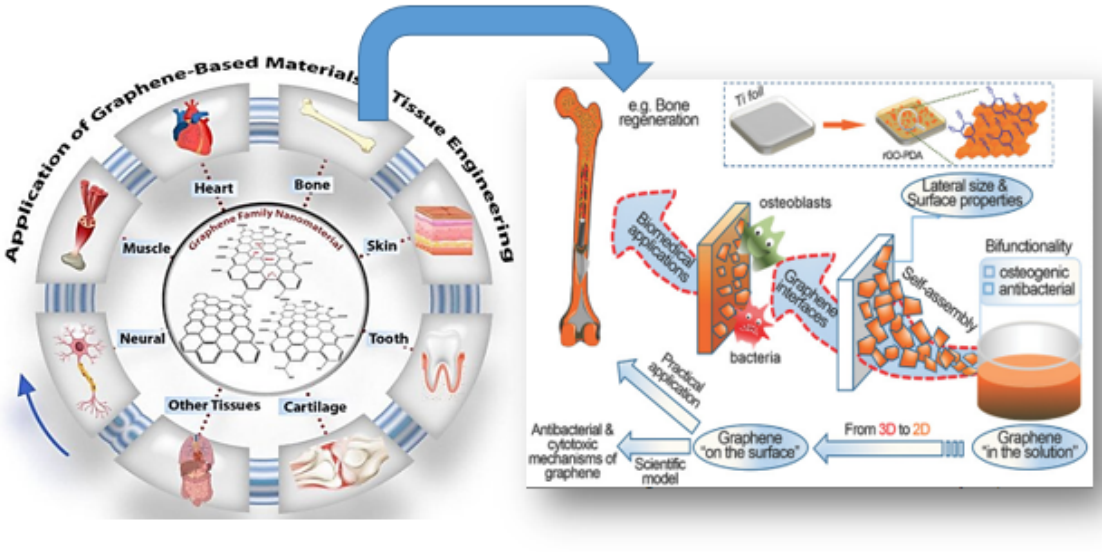

Figure 1. Illustration of the Gns-Coated Osteogenic Implant and Its Processing (Karahan et al., 2018; Riley et al., 2021).

cal uses for GO, including medication loading and transport (Daniyal et al., 2020; Wang et al., 2020). Graphene' is a single sheet of carbon that has been hybridized with sp^2 in its honeycomb structure". Comprised of sp^2 hybridized carbon atoms connected by Van der Waals connections 0.142 nm long, it is a two-dimensional crystal. (Ganjoo et al., 2023; Mahmood et al., 2023). Several methods have been established for the creation of Gns, and they can be broadly categorized as either physical or chemical.

Mechanical exfoliation or direct liquid-phase exfoliation can be used to physically separate Gns layers beginning arranged graphite sheets by using van der Waals force disturbance (Manikandan and Lee, 2023; Sontakke et al., 2023). The production of goods incorporating graphene is accomplished by chemical processes, including chemical vapor deposition, epitaxial growth, chemical reduction of GO (Anghel et al., 2023; Obayomi et al., 2023; Yadav et al., 2023).

This study aimed to systematically establish Gns by using nontoxic and eco-friendly chemicals. The proposed technology's simplicity, scalability, and environmental friendliness could allow the mass production of Gns. In this study, the graphene family's medical and preclinical bone regeneration applications were highlighted. By using the MG63 human osteosarcoma cell line, which is a well-established cell line for researching osteoblast function, Gns was tested in vitro for Gram-negative and -positive antibacterial activities.

2. EXPERIMENTAL SECTION

2.1 Materials

Graphite powder purity 99% (40-100 μm) purchased "Glentham life science Co." from Germany. Glycine chemical formula "NH_2.CH.COOH" was supplied by Thomas Baker India Co., India. sulfuric acid "H_2SO_4" was provided by "LOBA Chemie," Maharashtra, India.

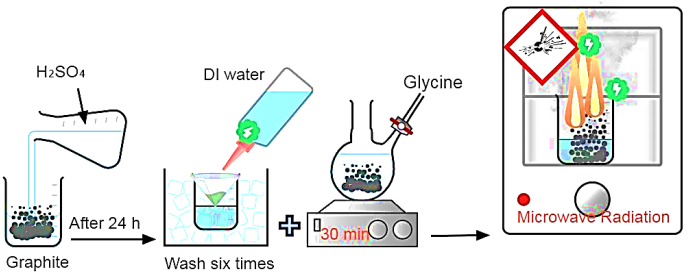

Figure 2. Gns Fabrication Scheme

2.2 Synthesis of Gns

Preparation of Gns show in Figure 2. Graphite powder (1 g) were immersed into 30 mL ice-cooled sulfuric acid from overnight. Glycine (0.5 g) was dissolved in distilled water over a magnetic hotplate stirrer (model SH-2) for 30 min. After being handled, the graphite flakes were filtered and allowed to dry naturally. Then, they were microwaved "Samsung, 2.45 GHz, 600 W, (105±5°C)" at 1 min to deliver a radiation thermal shock. Lightening and quick exfoliation of the precursors were the side effects of microwave irradiation. The reaction mixture was not subjected to longer periods or high microwave intensity to avoid severe explosions.

2.3 Characterization Techniques

X-ray diffraction "Shimadzu XRD-6000 "with Cu Ka radiation (λ) of 1.5406° A and scan angles of 2θ between 20° and 80°

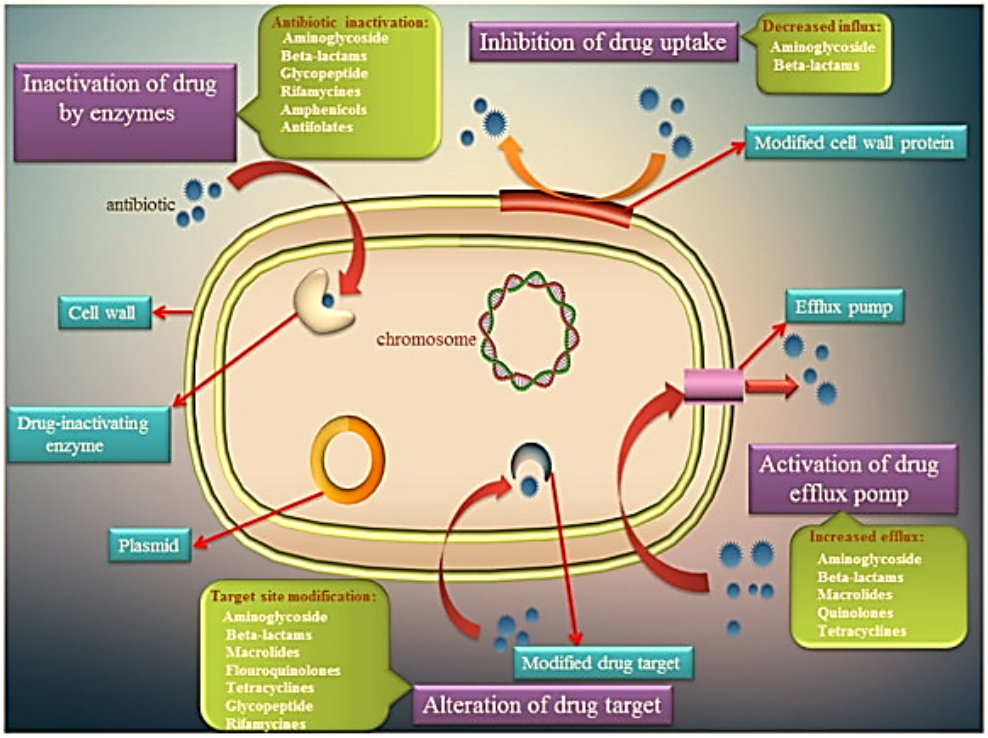

Figure 3. A Process that Contributes to the Evolution of Antibiotic Resistance in Cells (Yousefi et al., 2017)

was utilized for structural analysis of Gns, with a 0.02° step size and a rate of 5° (2) min^{-1}, to evaluate the form and crystallinity of Gns. Each specimen or species has one-of-a-kind XRD pattern, because identifying such content is as simple as comparing the achieved data with the database findings. XRD can be used to identify samples of graphite and graphene, even though it is not the best tool for spotting single-layer graphene. When evaluating a material's functional groups, Fourier transform infrared (FTIR) spectroscopy can be used because it provides a diagram connecting the permeability or absorption to the number of waves. The chemical configuration of Gns was determined using FTIR (Shimadzu, IRAffinity-1, Japan). Compressed KBr discs were used in the sample preparation process. The Gns absorption spectra varied between 400 and 4000 cm^{-1}. The visible and NIR optical transmission and absorption spectra (300-900 nm) of Gns were examined using a Shimadzu UV-Visible 1800 double beam spectrophotometer. A 532 nm argon laser (Bruker Senterra Raman microscope) with an incident laser power of 5 mW was used for Raman spectroscopy. TEM, JEM-2100F, Japan and FESEM, FEI NOVA NanSEM450 were used to analyze the morphology, shape, and size of the formed Gns; examine edge flaws; and determine layer thickness.

2.4 Anti-Bacterial Assay

The term "antimicrobial activity" refers to the effects of nanomaterials on the different growth stages of *P. aeruginosa* and *S. aureus*, including the naive, healthy-mature, and early-decline levels. Importantly, this study shows that the influence of physiological factors is not specific to a particular bacterial species or Gram-property. There are two possible modes of antibiotic resistance transmission: horizontal and vertical. Figure 3 shows several methods by which bacteria may become resistant to antibiotics. These include blocking the absorption of drugs, modifying antibiotic enzymes, changing target molecules, undergoing metamorphosis, sequestering drugs, and actively removing them from the cell. (Gungordu Er et al., 2023; Gurunathan et al., 2012; Karahan et al., 2018). The ability of Gram-negative organisms to survive in the presence of Gns was found to be significantly affected by the transition from exponential to stationary phase. Evidence from a battery of analyses of physiologically mature and immature cells' surface characteristics led to the hypothesis that the formation of the outer membrane structure was an important Cut wells of 4 mm in diameter were made in Mueller-Hinton agar plates, and 100 μl of indole and Gns stoke solutions were added to each. The negative control was composed of distilled water and DMSO. A series of well-dispersed Gns solutions (containing 15, 30, 45, and 60 $\mu g\ \mu L^{-1}$) were prepared by twofold serial dilution using nutrient broth as diluent. The inhibitory zone was calculated in millimeters after incubating the plates at 37°C for 18 to 24 hours. A shaker incubator was used to maintain the pathogens at 37°C overnight while they were cultivated in nutrient broth media.

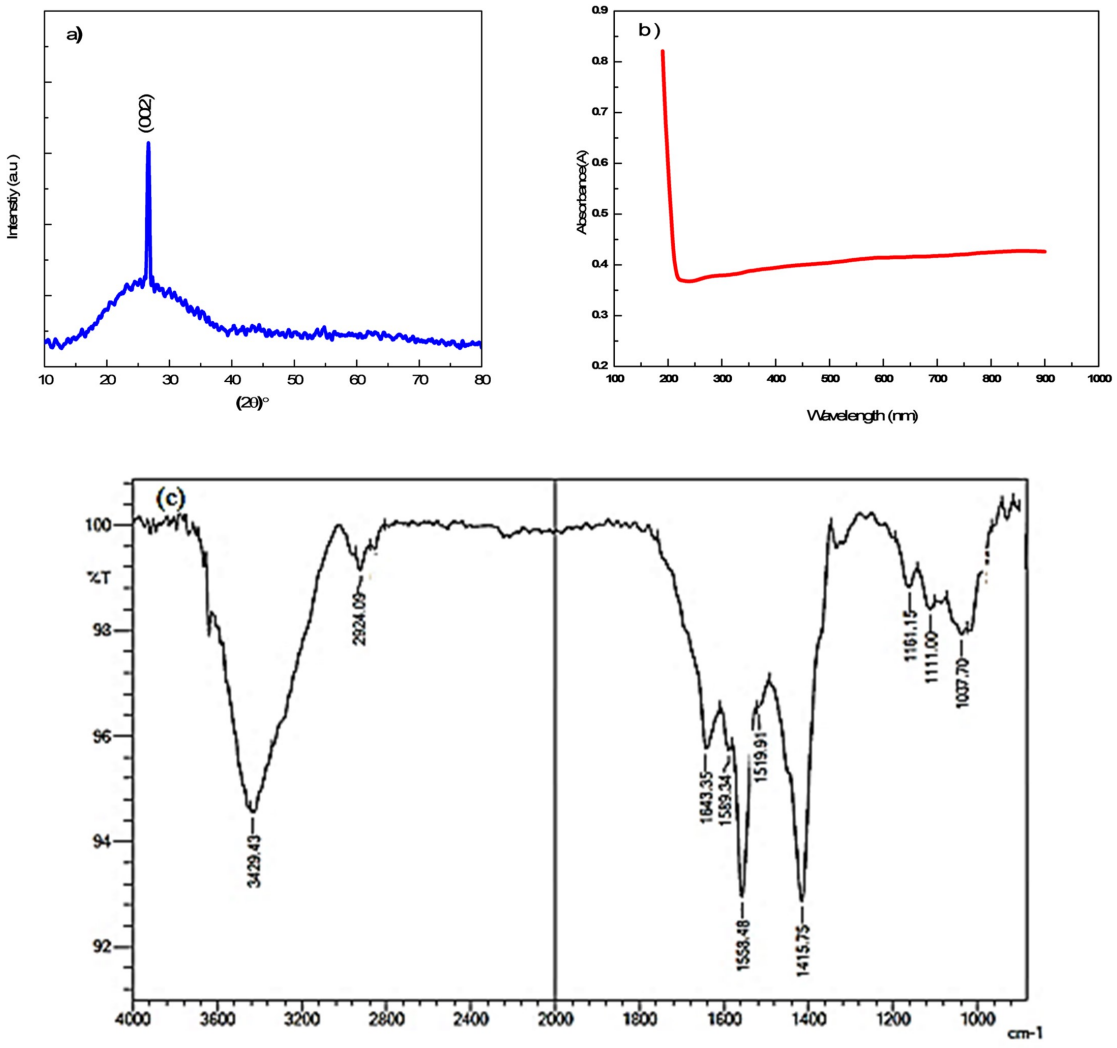

Figure 4. Characterization of Gns: a. XRD Patterns, b. UV–Visible Absorption Spectra, c. FTIR Spectra.

2.5 Cytotoxicity Assay

In this assay, the MG63 cell line was 37°C and 5% CO_2 was mixed with air to keep the cells alive. Dulbecco's Modified Eagle Medium (DMEM; Gibco, Life Technologies, Waltham, MA, USA) with 10% FBS and 1% PSF was supplied to the cells (Esmaeilnejad et al., 2023). At 75% confluence, the cells were separated in PBS (37°C) containing 0.25% trypsin (Gibco, Invitrogen, Waltham, MA, USA) and 0.1% ethylenediaminetetraacetic acid (Merck, Darmstadt, Germany). The cells were subsequently suspended in DMEM supplemented with 10% FBS and 1% PSF. Before the experiments, 96-well plates were seeded with cells at a density of 5,000 cells per well and incubated for 24 h. After being rinsed in phosphate-buffered saline (PBS; pH 7.4), the cells were cultured in new media containing the samples at various concentrations (50, 62.5, 125, 250, and 500 µg/mL). 3-(4,5-Dimethylthiazol-2-yl)-2, 5-diphenyltetrazolium bromide (MTT) dye reduction assay was performed to determine whether the cells were still alive. Cytotoxicity was evaluated using MTT at different sample concentrations. Following 72 h of incubation (37°C, 5% CO_2 in a humid atmosphere), MTT (0.5 mg/mL in PBS) was applied to each well, which was then incubated for 4 h at 37°C. Then, 100 mL DMSO was used to dissolve the resultant formazan before its absorbance was measured at 570 nm by using an ELISA reader. The data presented were the average of three separate tests. The concentrations of the samples at which 50% of the cells were killed were determined (IC_{50} values) as follows Equation (1) (Tasdemir et al., 2023):

$$\text{Cell Viability (\%)} = \frac{\text{Absorbance of the Medium of Treated Cells}}{\text{Absorbance of the Medium of Control}} \times 100\% \quad (1)$$

3. RESULTS AND DISCUSSION

3.1 X-Ray Diffraction" XRD "

An analysis of Gns's crystallinity and structure was performed using XRD. XRD exhibits a unique pattern, akin to a fingerprint, that is specific to each species, because identifying such content is as simple as comparing the achieved data with the database findings (Balqis et al., 2023; Zhang et al., 2000). XRD can be used to identify samples of graphite and graphene, even though it is not the best tool for spotting single-layer graphene. A base reflection (002) peak at 2θ = 26.6° (d spacing = 0.335 nm) is seen in pure graphite when an XRD pattern is used, as stated in (JCPDS, 75-1621) (Smith et al., 2019). Small peaks were detected in the XRD pattern of Gns, as shown in Figure 4 (a). The structure of Gns was affected probably because of the residual functional groups on the Gns sheets. Converting natural graphite to Gns breaks interplanar carbon bonds and reduces its crystalline size, as shown by a drop in intensity and a broadening of the peak. Oxygen-based functional compounds, for instance epoxy, carbonyl, hydroxyl, and carboxyl groups, in nanosheet layers increase Gns d-spacing. Moreover, structural flaws from sp^3 bonding on graphite flakes contribute to this phenomenon. In accordance with the Debye Scherrer Equation (2), the Gns d-spacing was determined to be 0.9 nm by using the following equation, where K is Scherrer's constant, the X-ray source's wavelength, β is the peak widening (FWHM) in radians, and the diffraction angle in degrees (Akin et al., 2024).

$$D = \frac{K\lambda}{\beta cos\theta} \quad (2)$$

3.2 UV-Vis Spectrophotometer

Figure 4 (b) displays the absorbance spectrum obtained from measuring Gns with a UV-Vis spectrophotometer. For Gns, there was only one peak in the absorbance results, and it was at around 200, where the electronic transition between orbitals peaks out. The orbital change can be linked to this peak. The peak at 200 nm is caused by aromatic C−C bond ($\pi-\pi\cdot$) transitions. According to previous research, the $\pi-\pi\cdot$ transition peaks can move to different locations of the energy spectrum depending on the distribution (type and number) of oxygenated functional groups on the Gns superficial (Faria et al., 2018). Absorbance spectra of Gns have this distinctive peak. The absorbance is constant at longer wavelengths, much like pure monolayer graphene.

3.3 Infrared Spectroscopy Using the Fourier Transform (FT-IR)

Figure 4 (c) displays the FT-IR spectrum of the finished Gns. The stretching vibrations of O−H atoms produce a wide peak around 3400 cm^{-1} group and 1415 cm^{-1} were seen as a result of the O−H bond stretching and bending vibrations from the (OH) functionality of Gns, while the peak at 2924.64 cm^{-1} was the characteristic peak of C−H stretching, validating the carbon-hydrogen functionalities in Gns. Gns also exhibit C−OH stretching vibrations and C−O stretching vibrations, as seen by the peaks at 1161 cm^{-1} and 1037 cm^{-1}, respectively. In addition, the (C=C) bond peaks at 1634 cm^{-1} in the FTIR spectra of ovalbumin-reduced graphene indicate skeletal vibrations of the unoxidized graphite domain, and the amide I and II peaks at 1558 cm^{-1}, respectively, indicate amides I and II, mainly for C=O stretching (Alsunbul et al., 2023; Convertino et al., 2023). The oxygen functionalities on the Gns have been removed, creating ovalbumin-functionalized graphene, and the amine group in ovalbumin amino acids reacts with graphene oxide epoxy group (Zak and Hashim, 2023).

3.4 Raman Spectra

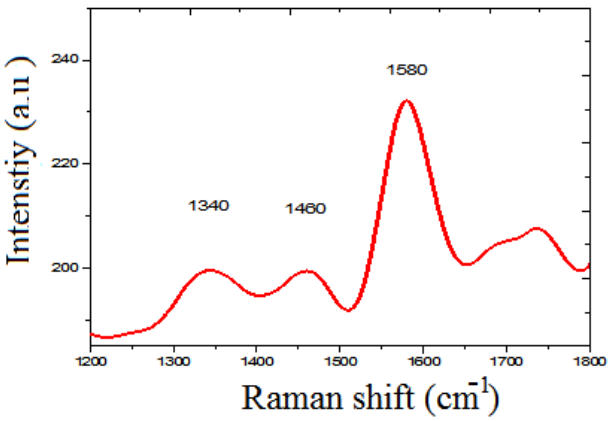

Figure 5. Raman spectra of Gns

The interaction between photons that cause excitation and the vibrations of molecular bonds leads to a change in the energy of the scattered photons. The phenomenon of energy shift observed in this context is commonly referred to as the Raman shift (Thyr and Edvinsson, 2023). This shift is a distinctive attribute of bond vibrations and serves as a unique identifier, allowing for the identification and characterization of underlying materials and structures (Strankowski et al., 2016). Graphite, diamond, fullerene, graphene, carbon nanotubes, and amorphous carbon may be identified by their Raman shifts from (lengthy to short) range crystalline vibrations molecular (Aswathappa et al., 2024). Figure 5 illustrates the presence of fundamental vibrations within the frequency range of (1100-1700) cm^{-1} for Gns. The D vibration band, arising beginning the A1g symmetry breathing mode of j-point photons, was observed at a wavenumber of 1340.31 cm^{-1} for Gns. Conversely, the G vibration band arising from the first-order scattering of E2g phonons by sp^2 carbon was seen at a wavenumber of 1580.19 cm^{-1} for Gns. In addition, the G vibration band is influenced by the stretching of the C−C bond, a characteristic feature found in all sp^2 carbon structures (Moseenkov et al., 2023). The bands observed in the Raman spectra, as depicted in Figure 5, can be identified as the D and G bands, which are commonly associated with disorder and tangential modes, re-

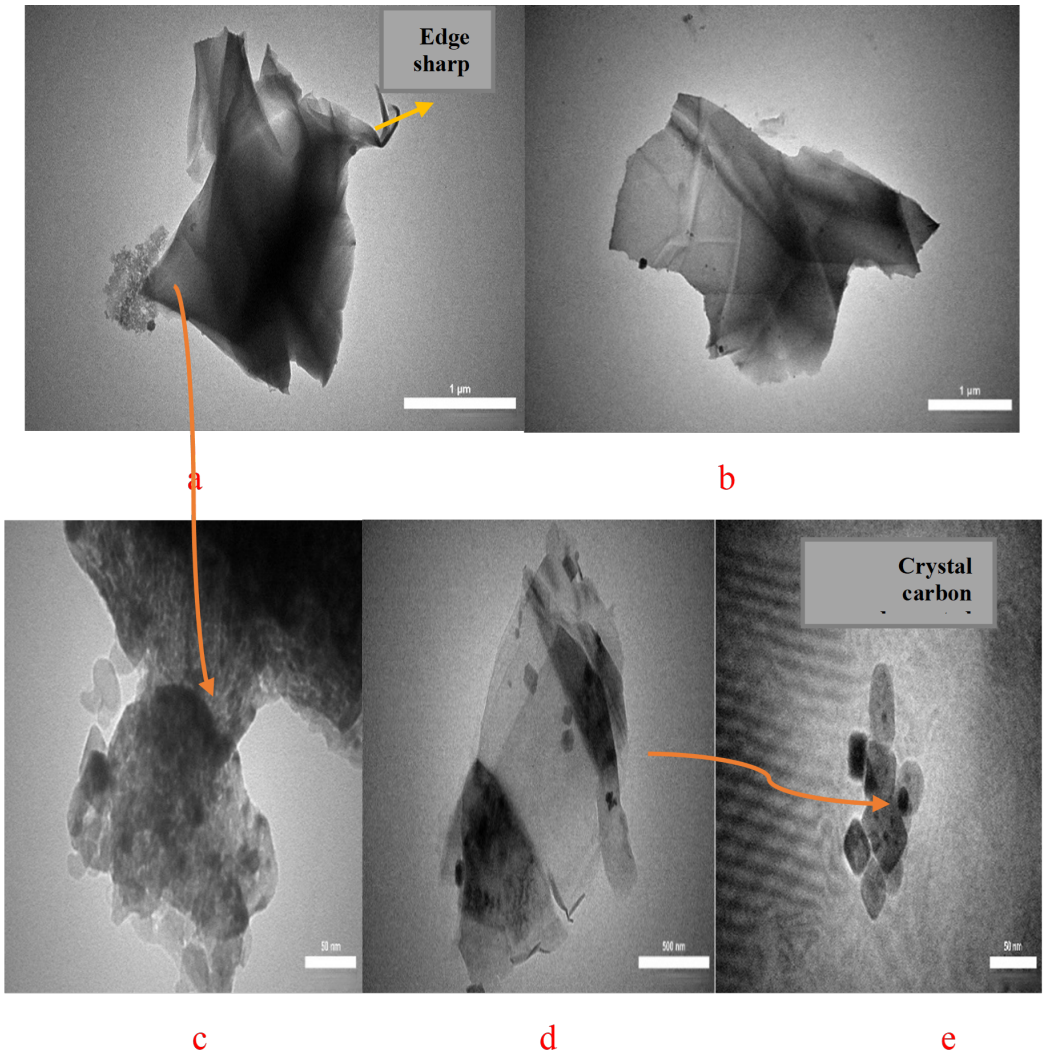

Figure 6. TEM Images of Gns.

spectively. Overall, this finding is consistent with the increased sp^2 character in the activated carbon. The local crystallinity of both forms of carbon is similar to that of graphite (Tan et al., 2023). The influence of the broadening on the peaks' finer sizes is visible. Defect locations were found on the "graphite-like sheets", through a pentagonal pinch vibration mode observed at 1460 cm^{-1}. The relative intensity ratio of ID/IG, which was determined after oxidation, was 0.85. Gns is not strictly a sp^2 framework, but rather a highly dispersed one with a significant sp^3 component. Despite the typical sp^2 materials, reducing defects in Gns could lead to an increase in the D/G ratio because of the increased number in sp^2 carbon particles surrounding the defects.

3.5 TEM Analysis

Demonstrates Gns quality and morphology, TEM was used. This suspension contains well-exfoliated Gns, including multilayers and monolayers with large sheets Figure 6. A graphene sheet with a single layer and a single, flat flake is shown in Figure 6 (a), (b). The high-resolution TEM photo in Figure 6 (a) shows graphene monolayers in multiple survey flakes. Figure 6 (b) shows a small number of layers, with clearly defined edges and sharp corners formed by the nanosheets. Reassembling is difficult for reduced Gns due to their corrugated shape, which is clear in Figure 6 (c). Its wrinkled shape is due to its high aspect ratio, which spans several hundred nanometers while being only a few nanometers thick. The surface of the Gns was adsorbed with some carbon nanoparticles. We got Gns and aggregative carbon nanoparticles, whose carbon nanoparticles decorated Gns in Figure 6 (d), (e).

3.6 FE-SEM Analysis

The FE-SEM image shows a porous network with clearly defined three-dimensional features, much like a layered sheet. The image analysis revealed both opaque and translucent regions. Dark spots on items' surfaces can be caused by a combi-

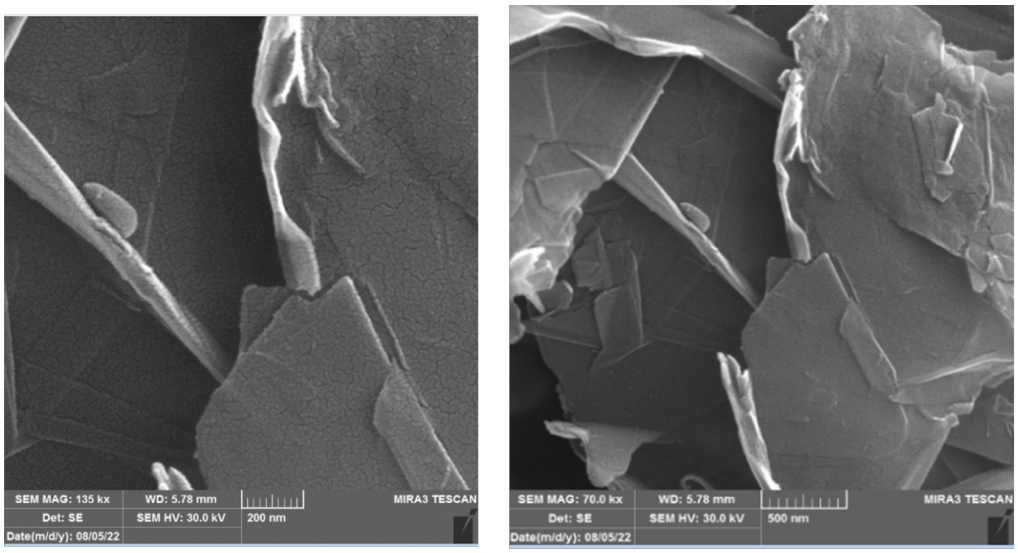

Figure 7. FESEM Images of Gns

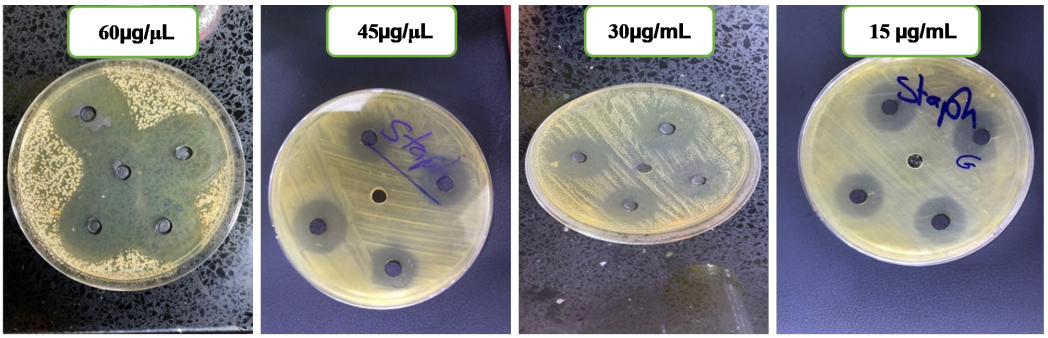

a- *Staphylococcus aureus*

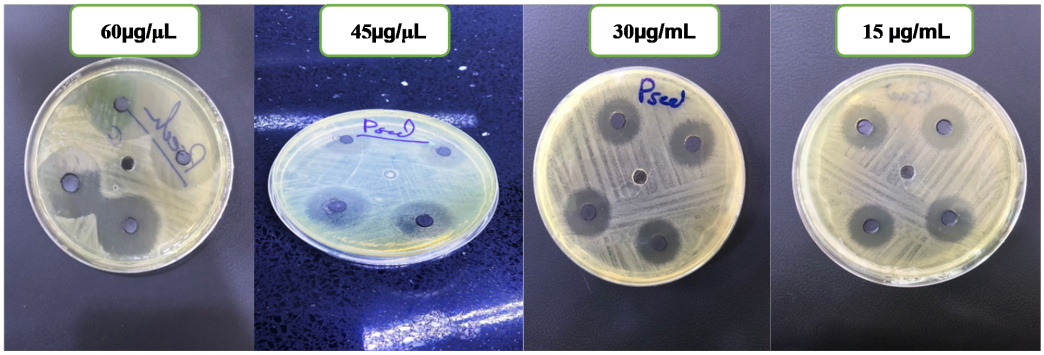

b- *Pseudomonas aeruginosa*

Figure 8. Antibacterial Activity of Gns

nation of graphene sheets, graphite, and oxygen groups from graphene oxide. Areas of very thin graphene layers are transparent. The more see-through something is, the thinner its sheets or the fewer oxygen groups it contains. Figure 7 depicts

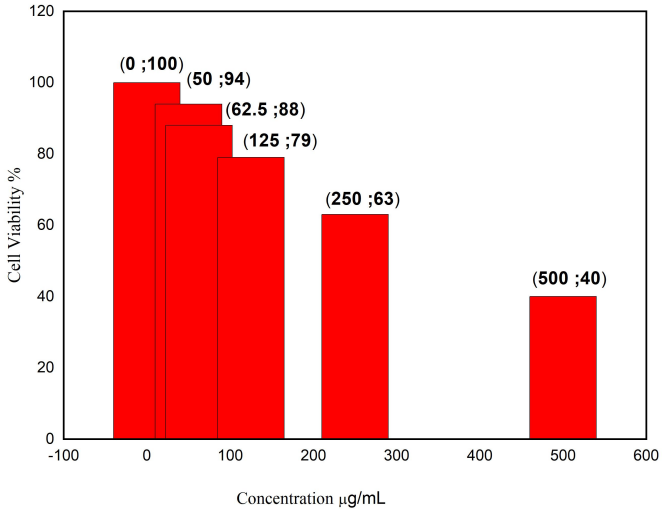

Figure 9. MTT Assay Was Used to Examine the Effects of Varying Concentrations of Gns on the Viability of MG63 Cells

Gns, which reveal solid sheets with a glossy surface and dense layers ranging in thickness from a few nanometers to 30nm. Each layer of nanosheets has a distinct corner. Figure 9 shows a flawless sheet with no visible flaws on its surface.

3.7 Activity of Gns Against Bacteria

To test for antibacterial activity in Figure 8, we used the agar well diffusion technique using Gns. *Staphylococcus aureus* and *Pseudomonas aeruginosa*, two common human pathogens, were used to investigate the antibacterial properties of Gns. Inhibitory activity data were collected at (15, 30,45, and 60) μg/mL after incubation at 37°C for 24 hours. Gns inhibition zone is displayed in Table 1. Graphene's antibacterial efficacy is strongly affected by its physicochemical features, including sheet size, layer number, oxidative stress mediation, and surface modifications. Byproducts of Gns are selected aimed at their biocidal action based on additional physicochemical parameters, such as temperature, exposure period, and concentration/dose (Gupta et al., 2024). Gns has oxygen functional groups on its edges and basal planes, but pure graphene doesn't. This makes a mix of sp^2 and sp^3 carbon domains that are hybridized. Various hydrogen-containing functional groups, for instance hydroxyl, ether, and carboxylic acid groups, and the number of water molecules interspersed between the oxidized sheets might change. Hydrophobic Gns stack. Microbes adsorb quickly and strongly on hydrophobic surfaces and reversibly adhere to hydrophilic substrates (Liu et al., 2020). Thus, bacteria's surface interactions will depend on their chemical composition. The surface charge can also affect bacterial adhesion. In addition to these varying chemical compositions, graphene-based materials also display structural differences in sheet size, from the micrometer to the nanoscale range. nanosheets, physically damaged cell membranes cause nucleus components to seep out and the membranes to lose their integrity. Also, the bacterial cell wall could be subject to oxidative damage (Azizi-Lalabadi et al., 2020). The two basic pathways by which oxidative stress manifests are those that rely on reactive oxygen species (ROS) and those that do not. Once again, the existence of radical species in the system causes stress owing to oxidation, which in turn ruptures the cell membrane and causes cell injury (Romero-Vargas Castrillon et al., 2015). Cell death follows lysis and occurs as a result of the release of cell components. showing that Gns has promising antibacterial properties. Researchers found that the synthesized Gns had sharp edges that could be used as "nano knives" in a FESEM and TEM analysis. When it this comes into contact with the outer surface of a bacterium, it has the potential to pierce through the cell wall and membrane (Hada et al., 2023; Ravikumar et al., 2022).

Table 1. Gns Varied Concentrations of Two-Bacterial Inhibitory Zone

S.NO	Concentrations (μg/mL)	Zone of Inhibition (mm)		
		P. aeruginosa	*S. aureus*	Control
1	15	18	17	0
2	30	23.6	20	0
3	45	26	24	0
4	60	33	30	0

3.8 Cell Viability

This study mainly aimed to demonstrate the comparable biocompatibility of Gns. MTT assay was used to determine if the material produced was able to kill osteoblast-like MG-63 cells in a lab setting and still be alive after 72 hours show in Figure 9. In accordance with ISO 10993-5, the decrease was examined using a colorimetric experiment to investigate the metabolic activity of mitochondrial dehydrogenase (Malhotra et al., 2022; Mohammed et al., 2020). The vitality of MG63 cells varied greatly depending on the Gns dose (50, 62, 125, 250, and 500 μg/mL) used in the incubation. After 72 hours of treatment, the MTT assays showed decreased cell viability with increasing concentration. Most members of the carbon family tend to congregate in physiological fluids because of electrostatic charges and nonspecific protein interactions owing to the oxygen- containing groups on its surface (Heister et al., 2010; Ilie et al., 2022). Gns is more biocompatible and hydrophilic. However, some research indicated that an overabundance of Gns may increase the production of ROS, which may result in cell death. Moreover, synthetic Gns with lower oxygenation produced significantly more ROS than those with higher oxygenation. Ionic forces and protein adsorption can affect cell adhesion to surfaces due to surface chemistry and roughness (Das et al., 2013; Gohari et al., 2021; Peng et al., 2017). So, using different varieties of graphene as a base could make the surface rougher, which could speed up cell division. Oxygen-containing groups on Gns are better at binding proteins than other graphene derivatives because they have a larger surface area, interact with molecules, and have surface flaws

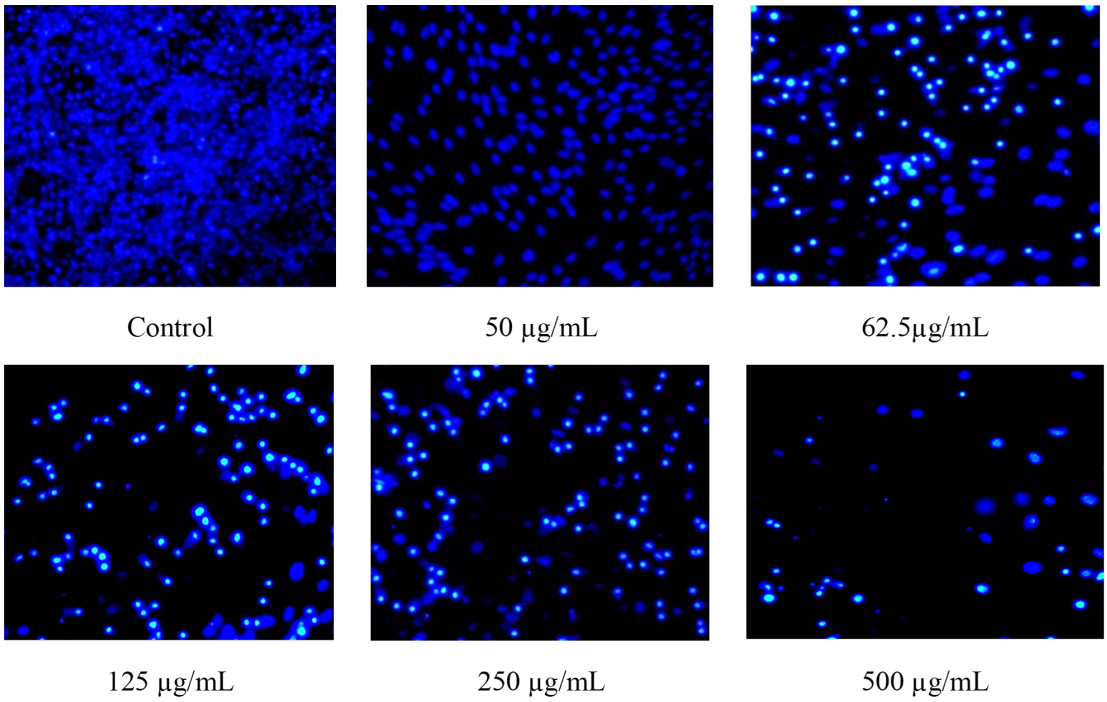

Figure 10. Fluorescence Images of MG63 Cells of Gns after 72 Hours at Various Doses.

that can serve as binding sites for proteins that help cells stick together and stay alive (Riss et al., 2004; Sylvester, 2011). Gns with more acute edges explained in Figure 6 (a), (b) interact with cell membranes more forcefully, which may result in more rupture and permeability of the membrane. Damage to DNA, alterations to proteins, and lipid peroxidation are just a few of the many cellular damage pathways associated with oxidative stress, which in turn impacts cell viability when ROS levels are high (Heister et al., 2010; Ilie et al., 2022).

The behavior of MG-63 cells exposed to varying doses of Gns was examined using fluorescence microscopy. At various doses of Gns, fluorescent pictures depicting cell attachment are shown in Figure 10. After 72 hours of cell culture on the material, the fluorescence images proved that the cells were alive. Many cells adhered strongly to the surface layers, and upon seeding, the morphology of all the specimens was consistent. Results were comparable to the control, suggesting that all of the prepared specimens, particularly Gns under (IC_50=490 μg/mL) calculated from Equation (1), provide a biocompatible environment for good cell attachment.

4. CONCLUSION

Graphite can be treated with microwaves to create two types of carbon nanomaterials with a single atomic layer: Gns nanosheets and carbon nanoparticles. Analysis using XRD, FT-IR, UV, and Raman verified the production of Gns. The FE-SEM and TEM revealed the multi-layer configuration of the Gns structures. Gns and carbon nanoparticle formations were revealed to have a layered layout by FE-SEM and TEM. As further proof of the layered structure and sheet folding, the Gns layers were extremely thin sheets. Antibacterial activity testing revealed that the produced Gns-decoration carbon nanoparticle was quite effective against the tested bacterial species. The MTT assay results that were previously reported provided evidence that the specimens that were tested were compatible with the MG-63 cells, which are representative of body cells. The MTT experiment found that the amount of Gns in the solution significantly affected the degree of mediated toxicity, with lower concentrations of Gns resulting in more toxic sheets. The cells' survival rate was straight connected to the concentration of surface functional groups. Toxic effects were shown to be mediated by inducing ROS generation within the cell. Our study introduces a novel materials approach to investigate the development of a synthetic structure for tissue engineering scaffold technology with potential applications in healthcare and biomedicine. This systematic discussion focuses on the physical and biological features of a graphene biomedical scaffold, ranging from low-scale to high-scale percentages of graphene. Research on biomedical scaffolds can serve as a valuable point of reference for future studies on bones and teeth. These biomedical scaffolds may be rapidly, effortlessly, and inexpensively produced and can serve as a benchmark for minimizing future research expenses.

5. ACKNOWLEDGMENT

We would like to thank College of Science, Diyala University for to help me with the measurements. Thank you to the Hassan Specialized Pathological Analysis Laboratory Research

Center. Thanks and gratitude to Dr. Asmaa Yahya Al-Jumaily Pathological Analysis Specialist for the biological analysis.

REFERENCES

Akin, M., M. Bekmezci, R. Bayat, I. Isik, and F. Sen (2024). Ultralight Covalent Organic Frame Graphene Aerogels Modified Platinum-Magnetite Nanostructure for Direct Methanol Fuel Cell. *Fuel*, **357**; 129771

Alsunbul, H., Y. F. Alfawaz, E. M. Alhamdan, I. Farooq, F. Vohra, and T. Abduljabbar (2023). Influence of Carbon and Graphene Oxide Nanoparticle on the Adhesive Properties of Dentin Bonding Polymer: A SEM, EDX, FTIR Study. *Journal of Applied Biomaterials & Functional Materials*, **21**; 22808000231159238

Anghel, E., B. Adiaconita, I. Demetrescu, and A. Avram (2023). A Review of Vertical Graphene and Its Biomedical Applications. *Coatings*, **13**(4); 761

Aswathappa, S., L. Dai, S. J. D. Sathiyadhas, M. B. D. S. Amalapushpam, M. Vijayan, I. Kim, R. S. Kumar, and A. I. Almansour (2024). Acoustic Shock Wave-Induced Short-Range Ordered Graphitic Domains in Amorphous Carbon Nanoparticles and Correlation Between Magnetic Response and Local Atomic Structures. *Diamond and Related Materials*, **141**; 110587

Azizi-Lalabadi, M., H. Hashemi, J. Feng, and S. M. Jafari (2020). Carbon Nanomaterials Against Pathogens; The Antimicrobial Activity of Carbon Nanotubes, Graphene/Graphene Oxide, Fullerenes, and Their Nanocomposites. *Advances in Colloid and Interface Science*, **284**; 102250

Balqis, N., B. Mohamed Jan, H. Simon Cornelis Metselaar, A. Sidek, G. Kenanakis, and R. Ikram (2023). An Overview of Recycling Wastes into Graphene Derivatives Using Microwave Synthesis; Trends and Prospects. *Materials*, **16**(10); 3726

Convertino, D., M. L. Trincavelli, C. Giacomelli, L. Marchetti, and C. Coletti (2023). Graphene-Based Nanomaterials for Peripheral Nerve Regeneration. *Frontiers in Bioengineering and Biotechnology*, **11**; 1306184

Daniyal, M., B. Liu, and W. Wang (2020). Comprehensive Review on Graphene Oxide for Use in Drug Delivery System. *Current Medicinal Chemistry*, **27**(22); 3665–3685

Das, S., S. Singh, V. Singh, D. Joung, J. M. Dowding, D. Reid, J. Anderson, L. Zhai, S. I. Khondaker, and W. T. Self (2013). Oxygenated Functional Group Density on Graphene Oxide: Its Effect on Cell Toxicity. *Particle & Particle Systems Characterization*, **30**(2); 148–157

Esmaeilnejad, A., M. T. Ardakani, M. Shokri, N. H. Khou, and M. Kamani (2023). Comparative Evaluation of the Effect of Two Platelet Concentrates (a-PRF and L-PRF) on the Cellular Activity of Pre-Osteoblastic MG-63 Cell Line: An In Vitro Study. *Journal of Dentistry*, **24**(2); 235

Faria, A. F., F. Perreault, and M. Elimelech (2018). Elucidating the Role of Oxidative Debris in the Antimicrobial Properties of Graphene Oxide. *ACS Applied Nano Materials*, **1**(3); 1164–1174

Ganjoo, R., S. Sharma, and A. Kumar (2023). Activation of Carbon Allotropes Through Covalent and Noncovalent Functionalization: Attempts in Modifying Properties for Enhanced Performance. In *Carbon Allotropes and Composites: Materials for Environment Protection and Remediation*. pages 31–50

Gohari, P. H. M., M. H. Nazarpak, and M. Solati-Hashjin (2021). The Effect of Adding Reduced Graphene Oxide to Electrospun Polycaprolactone Scaffolds on MG-63 Cells Activity. *Materials Today Communications*, **27**; 102287

Gungordu Er, S., M. Edirisinghe, and T. A. Tabish (2023). Graphene-Based Nanocomposites as Antibacterial, Antiviral and Antifungal Agents. *Advanced Healthcare Materials*, **12**(6); 2201523

Gupta, P. C., N. Sharma, S. Rai, and P. Mishra (2024). Use of Smart Silver Nanoparticles in Drug Delivery System. In *Metal and Metal-Oxide Based Nanomaterials: Synthesis, Agricultural, Biomedical and Environmental Interventions*. Springer, pages 213–241

Gurunathan, S., J. W. Han, A. A. Dayem, V. Eppakayala, and J. Kim (2012). Oxidative Stress-Mediated Antibacterial Activity of Graphene Oxide and Reduced Graphene Oxide in *Pseudomonas Aeruginos*a. *International Journal of Nanomedicine*, **7**; 5901–5914

Gürünlü, B., C. Tasdelen-Yücedag, and M. Bayramoglu (2022). One Pot Synthesis of Graphene Through Microwave Assisted Liquid Exfoliation of Graphite in Different Solvents. *Molecules*, **27**(15); 5027

Hada, V., K. Chaturvedi, A. Singhwane, N. Siraj, A. Gupta, N. Sathish, J. Chaurasia, A. Srivastava, and S. Verma (2023). Nanoantibiotic Effect of Carbon-Based Nanocomposites: Epicentric on Graphene, Carbon Nanotubes and Fullerene Composites: A Review. *3 Biotech*, **13**(5); 147

Heister, E., C. Lamprecht, V. Neves, C. Tîlmaciu, L. Datas, E. Flahaut, B. Soula, P. Hinterdorfer, H. M. Coley, and S. R. P. Silva (2010). Higher Dispersion Efficacy of Functionalized Carbon Nanotubes in Chemical and Biological Environments. *ACS Nano*, **4**(5); 2615–2626

Ilie, N., N. E. Serfoezoe, D. Prodan, J. Diegelmann, and M. Moldovan (2022). Synthesis and Performance of Experimental Resin-Based Dental Adhesives Reinforced with Functionalized Graphene and Hydroxyapatite Fillers. *Materials & Design*, **221**; 110985

Jia, Z., Y. Shi, P. Xiong, W. Zhou, Y. Cheng, Y. Zheng, T. Xi, and S. Wei (2016). From Solution to Biointerface: Graphene Self-Assemblies of Varying Lateral Sizes and Surface Properties for Biofilm Control and Osteodifferentiation. *ACS Applied Materials & Interfaces*, **8**(27); 17151–17165

Jiang, W.-S., C. Yang, G.-X. Chen, X.-Q. Yan, S.-N. Chen, B.-W. Su, Z.-B. Liu, and J.-G. Tian (2018). Preparation of High-Quality Graphene Using Triggered Microwave Reduction Under an Air Atmosphere. *Journal of Materials Chemistry C*, **6**(7); 1829–1835

Kang, E.-S., D.-S. Kim, I. R. Suhito, S.-S. Choo, S.-J. Kim, I. Song, and T.-H. Kim (2017). Guiding Osteogenesis of Mesenchymal Stem Cells Using Carbon-Based Nanomaterials. *Nano Convergence*, **4**; 1–14

Karahan, H. E., C. Wiraja, C. Xu, J. Wei, Y. Wang, L. Wang, F. Liu, and Y. Chen (2018). Graphene Materials in Antimicrobial Nanomedicine: Current Status and Future Perspectives. *Advanced Healthcare Materials*, **7**(13); 1701406

Li, X., A. H. Hirad, A. A. Alarfaj, H. Li, and R. Santhanam (2024). A Convergent Fabrication of Graphene Oxide/Silk Fibroin/Hydroxyapatite Nanocomposites Delivery Improved Early Osteoblast Cell Adhesion and Bone Regeneration. *Arabian Journal of Chemistry*, **17**(2); 105468

Liu, H., X. Liu, F. Zhao, Y. Liu, L. Liu, L. Wang, C. Geng, and P. Huang (2020). Preparation of a Hydrophilic and Antibacterial Dual Function Ultrafiltration Membrane with Quaternized Graphene Oxide as a Modifier. *Journal of Colloid and Interface Science*, **562**; 182–192

Mahmood, F., S. Ashraf, M. Shahzad, B. Li, F. Asghar, W. Amjad, and M. M. Omar (2023). Graphene Synthesis from Organic Substrates: A Review. *Industrial & Engineering Chemistry Research*, **62**(42); 17314–17327

Malhotra, R., C. Halbig, Y. Sim, C. Lim, D. Leong, A. Neto, S. Garaj, and V. Rosa (2022). Cytotoxicity Survey of Commercial Graphene Materials from Worldwide. *npj 2D Materials and Applications*, **6**(1); 65

Manikandan, V. and N. Lee (2023). Reduced Graphene Oxide: Biofabrication and Environmental Applications. *Chemosphere*, **311**; 136934

Mohammadrezaei, D., H. Golzar, M. Rezai Rad, M. Omidi, H. Rashedi, F. Yazdian, A. Khojasteh, and L. Tayebi (2018). In Vitro Effect of Graphene Structures as an Osteoinductive Factor in Bone Tissue Engineering: A Systematic Review. *Journal of Biomedical Materials Research Part A*, **106**(8); 2284–2343

Mohammed, H., A. Kumar, E. Bekyarova, Y. Al-Hadeethi, X. Zhang, M. Chen, M. Ansari, A. Cochis, and L. Rimondini (2020). Antimicrobial Mechanisms and Effectiveness of Graphene and Graphene-Functionalized Biomaterials: A Scope Review. *Frontiers in Bioengineering and Biotechnology*, **8**; 465

Moseenkov, S., V. Kuznetsov, N. Zolotarev, B. Kolesov, I. Prosvirin, A. Ishchenko, and A. Zavorin (2023). Investigation of Amorphous Carbon in Nanostructured Carbon Materials: A Comparative Study by TEM, XPS, Raman Spectroscopy and XRD. *Materials*, **16**(3); 1112

Obayomi, K., S. Lau, I. Mayowa, M. Danquah, J. Zhang, T. Chiong, L. Meunier, and M. Rahman (2023). Recent Advances in Graphene-Derived Materials for Biomedical Waste Treatment. *Journal of Water Process Engineering*, **51**; 103440

Peng, Z., X. Han, S. Li, A. Al-Youbi, A. Bashammakh, M. El-Shahawi, and R. Leblanc (2017). Carbon Dots: Biomacromolecule Interaction, Bioimaging and Nanomedicine. *Coordination Chemistry Reviews*, **343**; 256–277

Ravikumar, V., I. Mijakovic, and S. Pandit (2022). Antimicrobial Activity of Graphene Oxide Contributes to Alteration of Key Stress-Related and Membrane Bound Proteins. *International Journal of Nanomedicine*, **17**; 6707–6721

Riley, P., P. Joshi, H. Penchev, J. Narayan, and R. Narayan (2021). One-Step Formation of Reduced Graphene Oxide from Insulating Polymers Induced by Laser Writing Method. *Crystals*, **11**(11); 1308

Riss, T., R. Moravec, A. Niles, S. Duellman, H. Benink, T. Worzella, and L. Minor (2004). Cell Viability Assays Assay Guidance Manual. In *Assay Guidance Manual*. pages 1–23

Romero-Vargas Castrillon, S., F. Perreault, A. De Faria, and M. Elimelech (2015). Interaction of Graphene Oxide with Bacterial Cell Membranes: Insights from Force Spectroscopy. *Environmental Science & Technology Letters*, **2**(4); 112–117

Smith, A., A. LaChance, S. Zeng, B. Liu, and L. Sun (2019). Synthesis, Properties, and Applications of Graphene Oxide/Reduced Graphene Oxide and Their Nanocomposites. *Nano Materials Science*, **1**(1); 31–47

Sontakke, A., S. Tiwari, and M. Purkait (2023). A Comprehensive Review on Graphene Oxide-Based Nanocarriers: Synthesis, Functionalization and Biomedical Applications. *FlatChem*, **38**; 100484

Strankowski, M., D. Wlodarczyk, L. Piszczyk, and J. Strankowska (2016). Polyurethane Nanocomposites Containing Reduced Graphene Oxide: FTIR, Raman, and XRD Studies. *Journal of Spectroscopy*, **2016**(1); 7520741

Sumathra, M., K. Sadasivuni, S. Kumar, and M. Rajan (2018). Cisplatin-Loaded Graphene Oxide/Chitosan/Hydroxyapatite Composite as a Promising Tool for Osteosarcoma-Affected Bone Regeneration. *ACS Omega*, **3**(11); 14620–14633

Suresh, M. and A. Sivasamy (2018). Synthesis and Characterization of High Quality Nano Layered Reduced Graphene Oxide by Solvothermal Method and Its Antibacterial Activity. *Inorganic and Nano-Metal Chemistry*, **48**(4–5); 233–238

Sylvester, P. (2011). Optimization of the Tetrazolium Dye (MTT) Colorimetric Assay for Cellular Growth and Viability. In *Drug Design and Discovery: Methods and Protocols*. pages 157–168

Szunerits, S. and R. Boukherroub (2016). Antibacterial Activity of Graphene-Based Materials. *Journal of Materials Chemistry B*, **4**(43); 6892–6912

Tan, X., Y. Jiang, Q. Peng, T. Subrova, J. Saskova, J. Wiener, M. Venkataraman, J. Militky, P. Kejzlar, and A. Mahendran (2023). Development and Characterization of Silane Crosslinked Cellulose/Graphene Oxide Conductive Hydrophobic Membrane. *Cellulose*, **30**(7); 4561–4574

Tasdemir, S., Z. Morcimen, A. Doğan, C. Görgün, and A. Sendemir (2023). Surface Area of Graphene Governs Its Neurotoxicity. *ACS Biomaterials Science & Engineering*, **9**(2); 793–802

Thyr, J. and T. Edvinsson (2023). Evading the Illusions: Iden-

tification of False Peaks in Micro-Raman Spectroscopy and Guidelines for Scientific Best Practice. *Angewandte Chemie International Edition*, **62**(43); e202219047

Wang, B., S. Yuan, W. Xin, Y. Chen, Q. Fu, L. Li, and Y. Jiao (2021). Synergic Adhesive Chemistry-Based Fabrication of BMP-2 Immobilized Silk Fibroin Hydrogel Functionalized with Hybrid Nanomaterial to Augment Osteogenic Differentiation of rBMSCs for Bone Defect Repair. *International Journal of Biological Macromolecules*, **192**; 407–416

Wang, C., M. Song, X. Chen, D. Li, and W. Xia (2020). Synthesis of Few-Layer Graphene Flakes by Magnetically Rotating Arc Plasma: Effects of Input Power and Feedstock Injection Position. *Applied Physics A*, **126**; 1–13

Wang, J., H. Yin, X. Meng, J. Zhu, and S. Ai (2011). Preparation of the Mixture of Graphene Nanosheets and Carbon Nanospheres with High Adsorptivity by Electrolyzing Graphite Rod and Its Application in Hydroquinone Detection. *Journal of Electroanalytical Chemistry*, **662**(2); 317–321

Wu, M., L. Zou, L. Jiang, Z. Zhao, and J. Liu (2021). Osteoinductive and Antimicrobial Mechanisms of Graphene-Based Materials for Enhancing Bone Tissue Engineering. *Journal of Tissue Engineering and Regenerative Medicine*, **15**(11); 915–935

Yadav, A., H. Kumar, R. Sharma, and R. Kumari (2023). Synthesis, Processing, and Applications of 2D (Nano) Materials: A Sustainable Approach. *Surfaces and Interfaces*, **39**; 102925

Yousefi, M., M. Dadashpour, M. Hejazi, M. Hasanzadeh, B. Behnam, M. de la Guardia, N. Shadjou, and A. Mokhtarzadeh (2017). Anti-Bacterial Activity of Graphene Oxide as a New Weapon Nanomaterial to Combat Multidrug-Resistance Bacteria. *Materials Science and Engineering: C*, **74**; 568–571

Zak, A. and A. Hashim (2023). Synthesis, Characterization and Cytotoxicity Studies of Au-Decorated Graphene Oxide Nanosheets. *Ceramics International*, **49**(11); 18577–18583

Zare, P., M. Aleemardani, A. Seifalian, Z. Bagher, and A. Seifalian (2021). Graphene Oxide: Opportunities and Challenges in Biomedicine. *Nanomaterials*, **11**(5); 1083

Zhang, R., P. Thiyagarajan, and D. Tiede (2000). Probing Protein Fine Structures by Wide Angle Solution X-Ray Scattering. *Journal of Applied Crystallography*, **33**(3); 565–568

